Chinese Journal of Natural Medicines

Three rare anti-inflammatory sesquiterpene lactones from *Magnolia grandiflora*

Shuangyu XU, Feng ZHANG, Linlan TAO, Yangming JIANG, Tao HUANG, Yanan LI, Zhanxing HU, Jue YANG, Xiaojiang HAO, Chunmao YUAN

Citation: Shuangyu XU, Feng ZHANG, Linlan TAO, Yangming JIANG, Tao HUANG, Yanan LI, Zhanxing HU, Jue YANG, Xiaojiang HAO, Chunmao YUAN, Three rare anti-inflammatory sesquiterpene lactones from *Magnolia grandiflora*, Chinese Journal of Natural Medicines, 2024, 22(3), 265-272. doi: 10.1016/S1875-5364(24)60601-1.

View online: https://doi.org/10.1016/S1875-5364(24)60601-1

Available online at www.sciencedirect.com
ScienceDirect
Chinese Journal of Natural Medicines 2024, **22**(3): 265-272
doi: 10.1016/S1875-5364(24)60601-1
Chinese Journal of Natural Medicines

•Original article•

Three rare anti-inflammatory sesquiterpene lactones from *Magnolia grandiflora*

XU Shuangyu[1, 2, 3], ZHANG Feng[1, 2, 3], TAO Linlan[1, 2, 3], JIANG Yangming[1, 2, 3], HUANG Tao[1, 2, 3], LI Yanan[1, 2, 3], HU Zhanxing[1, 2, 3], YANG Jue[1, 2, 3], HAO Xiaojiang[1, 2, 3, 4*], YUAN Chunmao[1, 2, 3*]

[1] *State Key Laboratory of Functions and Applications of Medicinal Plants, Guizhou Medical University, Guiyang 550014, China;*
[2] *School of Pharmaceutical Sciences, Guizhou Medical University, Guiyang 550025, China;*
[3] *Natural Products Research Center of Guizhou Province, Guiyang 550014, China;*
[4] *State Key Laboratory of Phytochemistry and Plant Resources in West China, Kunming Institute of Botany, Chinese Academy of Sciences, Kunming 650201, China*

Available online 20 Mar., 2024

[ABSTRACT] Four new sesquiterpene lactones (SLs) (**1**–**4**), along with a biosynthetically related SL (**5**), have been isolated from the leaves of *Magnolia grandiflora*. Magrandate A (**1**) is notable as the first C18 homogemarane type SL, featuring a unique 1,7-dioxaspiro[4.4]nonan-6-one core. Compounds **2** and **3**, representing the first instances of chlorine-substituted gemarane-type SL analogs in natural products, were also identified. The structures of these isolates were elucidated through a combination of spectroscopic data analysis, electronic circular dichroism calculations, and X-ray single-crystal diffraction analysis. All isolates demonstrated anti-inflammatory activity in lipopolysaccharide-stimulated RAW264.7 cells. Notably, **3**–**5** showed a significant inhibitory effect on nitric oxide production, with IC_{50} values ranging from 0.79 to 4.73 μmol·L^{-1}. Additionally, **4** and **5** exhibited moderate cytotoxic activities against three cancer cell lines, with IC_{50} values between 3.09 and 11.23 μmol·L^{-1}.

[KEY WORDS] *Magnolia grandiflora*; Sesquiterpene lactones; Isolation and identification; Anti-inflammatory activity
[CLC Number] R284.1 **[Document code]** A **[Article ID]** 2095-6975(2024)03-0265-08

Introduction

Inflammatory responses are mediated by a series of chemical factors and constitute the body's automatic physiological defense mechanism. However, an excessive inflammatory response can lead to various diseases [1–4]. Clinically used anti-inflammatory drugs mainly fall into two categories: non-steroidal and steroidal anti-inflammatory drugs. These medications, however, are associated with numerous adverse reactions, including stomach bleeding and kidney issues [5]. Consequently, developing new anti-inflammatory drugs that are highly effective, low in toxicity, and have minimal or no side effects is of significant importance.

Natural products play a crucial role in drug discovery [6]. Sesquiterpenoid lactones (SLs), which consist of three isoprene units and a lactone group, are prevalent in several plant families, including Asteraceae [7], Orobanchaceae [8, 9], and Magnolia [10-12]. SLs are believed to originate from two primary precursors: isopentenyl diphosphate and dimethylallyl diphosphate [7]. Numerous SLs have demonstrated potent anti-inflammatory effects by inhibiting the activation of NF-κB, MAPKs, and STAT, making them promising natural compounds for combating inflammation [13]. Therefore, the exploration of SLs with notable anti-inflammatory activities has garnered substantial interest in the fields of natural product research, synthesis, and biology.

Magnolia grandiflora, belonging to the Magnolia family,

[Received on] 12-May-2023
[Research funding] This work was supported by the National Natural Science Foundation of China (Nos. 82060631 and 32270413), the Science and Technology Department of Guizhou Province [Nos. QKH JC(2020)1Z076 and QKH JC (2020)1Y400], the Cultivation Project of National Natural Science Foundation of Guizhou Medical University (No. 2023-106), the Outstanding Young Scientific and Technological Talents in Guizhou Province [No. QKH PTRC(2021)5633], High-level Innovative Talents in Guizhou Province (Thousand Levels of Talent for YUAN Chunmao in 2018), "Light of the West" Talent Cultivation Program of Chinese Academy of Sciences for YUAN Chunmao [RZ (2020)82], Guizhou Science and Technology Innovation Talent Team (No. QKHPTRC-CXTD[2022]007), and the Natural Science Foundation of Guizhou Province [No. QKHZYD(2022)4015].
[*]**Corresponding author]** E-mails: haoxj@mail.kib.ac.cn (HAO Xiaojang); yuanchunmao01@ 126.com (YUAN Chunmao)
These authors have no conflict of interest to declare.

is utilized in traditional Chinese medicine to treat conditions such as exogenous colds, headaches, nasal congestion, and hypertension [14]. Previous phytochemical studies on this plant have yielded a series of SLs with effective cytotoxic and anti-inflammatory activities [10, 15-17]. In an effort to discover new anti-inflammatory SLs from *Magnolia grandiflora* in Guizhou Province, China, we investigated the chemical constituents of this plant, which led to the identification of four new SLs (**1**–**4**) and a biosynthetically related SL (**5**) (Fig. 1). Notably, Magrandate A (**1**) is the first C18 homogemarane type SL with an unprecedented 1,7-dioxaspiro[4.4]nonan-6-one core, while **2** and **3** are the first chlorine-substituted parthenolide analogs. Analysis of the biogenic synthesis pathways suggests that **1**–**4** are derived from **5**, with varying epoxidized positions at $\Delta^{11,13}$ or $\Delta^{1,10}$ in **5**, leading to different structural types (**1**–**4**). Three compounds (**3**–**5**) showed greater potential in inhibiting NO production than the positive control, pyrrolidine dithiocarbamate. This paper details the isolation, structural elucidation, plausible biosynthesis pathway, and biological evaluation of these isolates.

Results and Discussion

The air-dried and pulverized leaves of *M. grandiflora* (30 kg) underwent extraction with 90% methanol (120 L × 3) under reflux, repeated three times. The MeOH extracts were concentrated under reduced pressure to yield a crude residue of 2.1 kg. Subsequent chromatographic separation of this extract yielded four new sesquiterpenes (**1**–**4**) along with a biosynthetically related sesquiterpene (**5**) (Fig. 1).

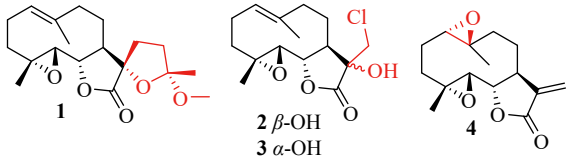

Fig. 1 Chemical structures of 1–4.

Magrandate A (**1**) was identified with the molecular formula $C_{19}H_{28}O_5$, as indicated by a HR-ESI-MS ion at *m/z* 359.1827 $[M + Na]^+$ (Calcd. for $C_{19}H_{28}O_5Na$: 359.1829), exhibiting six indices of hydrogen deficiency (IHDs). The ^{1}H NMR spectrum (Table 1) revealed the presence of four methyl groups (δ_H 1.28, s; 1.61, s; 1.70, s; 3.27, s) and an olefinic proton (δ_H 5.17, dd, J = 11.9, 2.1 Hz). Further analysis of the ^{13}C NMR data indicated the existence of a lactone carbonyl (δ_C 176.0) and a double bond (δ_C 125.0 and 134.9), accounting for two IHDs. Consequently, compound **1** likely possesses a four-ring system, as suggested by the remaining four IHDs.

Table 1 ^{1}H and ^{13}C NMR Data ($CDCl_3$, δ in ppm, J in Hz) for compounds 1–4

No.	1		2		3		4	
	δ_H	δ_C	δ_H	δ_C	δ_H	δ_C	δ_H	δ_C
1	5.17, dd (11.9, 2.1)	125.0	5.20, dd (12.0, 2.0)	124.8	5.19, dd (11.7, 2.1)	125.5	3.09, dd (9.4, 5.1)	58.8
2	2.38, m 2.18, m	24.0	2.40, m 1.99, m	24.1	2.38, m 2.17, m	24.1	2.35, m 1.57, m	23.9
3	2.15, m 1.23, m	37.0	2.15, m 1.24, m	36.8	2.13, m 1.21, m	36.7	2.27, m 1.37, m	32.9
4		61.7		62.0		62.2		60.1
5	2.71, d (9.1)	66.9	2.74, d (9.3)	66.5	2.74, d (9.0)	66.7	2.93, d (9.3)	64.0
6	3.75, t (9.5)	80.4	4.16, t (9.2)	82.8	4.13, t (9.5)	81.4	3.80, t (9.6)	81.5
7	2.43, m	50.5	2.48, t (8.6)	48.2	2.49, t (9.7)	53.0	2.85, m	45.8
8	2.06, m 1.46, m	25.0	2.19, m 1.59, m	24.0	2.04, m 1.79, m	24.4	2.03, m 1.52, m	25.1
9	2.36, m 2.05, m	41.2	2.32, q (6.7) 2.04, d (13.0)	41.1	2.38, m 2.10, m	41.5	2.04, m 1.89, m	38.4
10		134.9		135.1		134.5		60.7
11		87.4		78.0		78.0		139.0
12		176.0		174.7		176.0		169.1
13	2.32, m 1.81, m	28.3	3.82, d (11.5) 3.61, d (11.5)	43.1	3.68, dd (14.3, 11.6)	43.7	6.28, d (3.7) 5.57, d (3.3)	120.0
14	1.70, s	17.1	1.71, s	17.1	1.70, s	16.9	1.46, s	21.9
15	1.28, s	17.2	1.30, s	17.2	1.30, s	17.2	1.55, s	19.4
16	2.19, m 2.08, m	37.5						
17		109.4						
18	1.61, s	21.1						
OCH_3	3.27, s	48.9						

In the ^{1}H-^{1}H COSY spectrum (Fig. 2), three distinct fragments (a–c) were identified, as evidenced by the observed cross-peaks. Key HMBC (Heteronuclear Multiple Bond Correlation) correlations provided crucial insights into the structure. Specifically, correlations from methyl group Me-14 to carbons C-1, C-9, and C-10, and from Me-15 to C-3, C-4, and C-5, revealed pivotal connections. These correlations established a 10-membered carbon ring within the molecule. The presence of a typical 1,2-epoxy ring was deduced from the chemical shifts (δ_H 2.71, J = 9.1 Hz, δ_C 61.7 and 66.9). Further HMBC correlations, namely from H-7 to C-11 and C-12, complemented by an oxygenated methine carbon signal (δ_C 80.4), led to the identification of a γ-lactone ring. This finding suggests that compound **1** is a germacrane-type sesquiterpene. The structure was further elaborated through the identification of a novel spiro ring system. This system, inferred to be fused with the γ-lactone ring *via* C-11, was supported by critical HMBC correlations from H_2-13 to C-7, C-11, and C-12, and from Me-18 to C-16 and C-17. Additionally, two unconnected oxidized quaternary carbons (C-11 and C-17) with chemical shifts δ_C 87.4 and 109.4, respectively, supported this structure. The presence of a methoxy group attached to C-17 was inferred from HMBC correlations of the methoxy methyl group Me-19 to C-17. Accordingly, the planar structure of compound **1** was established based on these spectroscopic analyses and correlations.

In the Nuclear Overhauser Effect Spectroscopy (NOESY) (Fig. 2), the relative configuration of compound **1** was determined. The presence of cross-peaks between H-1/H-5, H-5/H-7, H-7/H-8α, H-8α/H-13α, and H-8α/OMe-19 indicated that these groups were co-facial and, by convention, assigned α-orientation. Conversely, the groups Me-14, Me-15, H-6, and H-13β were assigned β-orientated as suggested by their NOESY correlations of Me-14/Me-15, Me-15/H-6, and H-6/H-13β. The critical NOESY correlations between H-6/H-13β and H-8α/OMe-19 were instrumental in establishing the orientation of the spiro ring system. Consequently, the relative configuration of compound **1** was elucidated. The absolute configuration was assigned by electric circular dichroism (ECD) calculation with the time-dependent density functional theory (TDDFT) methodology at the CAM-B3LYP/TZVP level [18-20]. The absolute configuration was determined using ECD calculation, employing the TDDFT methodology at the CAM-B3LYP/TZVP level [18-20]. The calculated ECD spectra corresponded well with that of the (4*R*,5*S*,6*S*,7*R*,11*S*,17*R*)-**1** configuration (Fig. 3). Furthermore, the absolute configuration of compound **1** was corroborated by X-ray crystallography (Fig. 4) [21], providing a comprehensive understanding of its three-dimensional structure.

Magrandate B (compound **2**) was determined to have the molecular formula of $C_{15}H_{21}O_4Cl$, as indicated by high-resolution electrospray ionization mass spectrometry (HR-ESI-MS) with a peak at *m/z* 323.1015 $[M + Na]^+$ (Calcd. for $C_{15}H_{21}O_4ClNa$: 323.1021) and exhibited five IHDs. Analysis of its ^{1}H NMR data (Table 1) revealed two methyl groups (δ_H

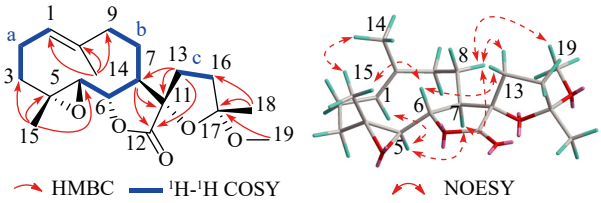

Fig. 2 Key 2D NMR correlations of 1.

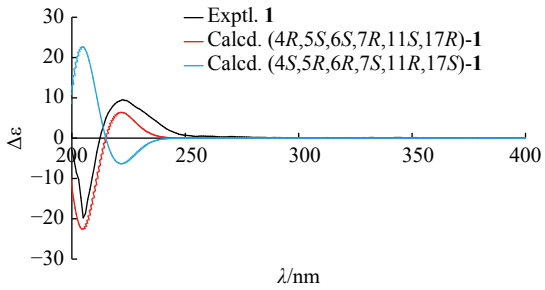

Fig. 3 Calculated and experimental ECD spectra of 1.

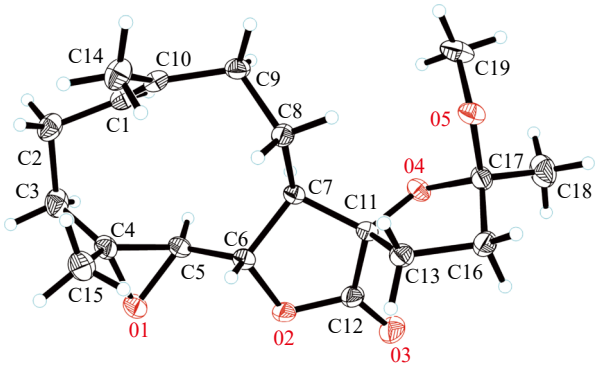

Fig. 4 X-ray crystallographic structure of 1 (CCDC: 2239027).

1.30, s; 1.71, s) and an olefinic proton (δ_H 5.20, dd, J = 12.0, 2.0 HZ). The ^{13}C NMR and HSQC (Heteronuclear Single Quantum Coherence) data indicated that the core structure of **2** consists of 15 carbons, including two methyls, five methylenes, four methines, and four quaternary carbons. Furthermore, the presence of a 1,2-epoxy ring was inferred from the chemical shifts (δ_C 62.0 and 66.5).

Comparison of the NMR spectroscopic data of compound **2** with those of compound **5** suggested that **2** is a germacranolide derivative with the same 10-membered carbon ring [14], γ-lactone ring, and 1,2-epoxy ring. A notable distinction between these two compounds is the presence of a chlorine atom at C-13 and an additional hydroxyl group at C-11 in compound **2**, as confirmed by HR-ESI-MS data and HMBC correlations from H_2-13 to C-7, C-11, and C-12 (Fig. 5). The relative configuration of **2** was elucidated from its NOESY spectrum; correlations of Me-14 with Me-15 and Me-15 with H-6 indicated β-oriented for these protons. Conversely, cross-peaks of H-1 with H-5, H-5 with H-7, and H-7 with H_2-13 suggested α-orientation for H-5, H-7, and the chloromethyl

group (Fig. 5). Thus, the relative configuration was conclusively assigned as depicted in Fig. 5. The absolute configuration of compound **2** was initially established by ECD calculation, with the red dashed curve in Fig. 6 suggesting the absolute configuration of (4*R*,5*S*,6*S*,7*R*, 1*R*)-**2**. Subsequently, X-ray crystallography of compound **2** provided definitive confirmation of this absolute configuration (Fig. 7).

Magrandate C (compound **3**) was determined to have the same molecular formula as magrandate B (compound **2**), as indicated by the HR-ESI-MS analysis. The one-dimensional (1D) and two-dimensional (2D) NMR data established that both compounds shared the same planar structure. A key difference was observed in the carbon chemical shift of C-7 (δ_C 48.2 for compound **2**; δ_C 53.0 for compound **3**), suggesting a different orientation of the γ-lactone ring in these compounds. This hypothesis was supported by NOESY correlations of Me-14 with Me-15, Me-15 with H-6, and H-6 with H_2-13, indicating a shift in the orientation of the chloromethyl group from α in compound **2** to β in compound **3**. According to the above data, the structure of compound **3** was identified (Fig. 1).

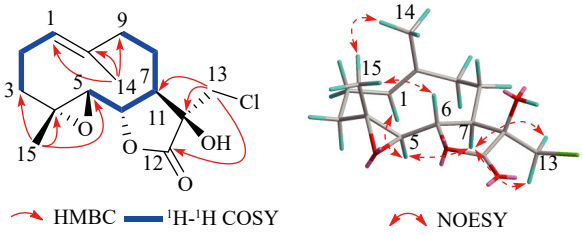

Fig. 5 key 2D NMR correlations of 2.

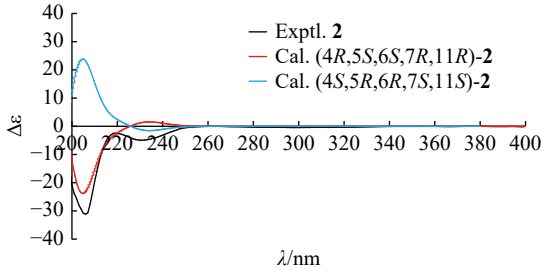

Fig. 6 Calculated and experimental ECD spectra of 2.

Magrandate D (compound **4**) was identified with the molecular formula $C_{15}H_{20}O_4$, as revealed by HR-ESI-MS, and exhibited six IHDs. The 1D NMR data suggested the presence of two characteristic 1,2-epoxy rings and an α,β-unsaturated γ-lacto). A comparison of the 1D NMR data between compound **4** and michelenolide [14] indicated similarities, with the exception of the orientation of the 1,10-epoxy ring. The NOESY spectrum was instrumental in establishing the relative configuration of compound **4**. Correlations of H-1 with Me-15, Me-15 with H-6, and H-6 with H-1 implied a β-orientation of those groups (Fig. 8). Conversely, the α-orientation was assigned to the protons of H-5, H-7, and Me-14, based on their NOESY correlations of H-7 with Me-14, Me-

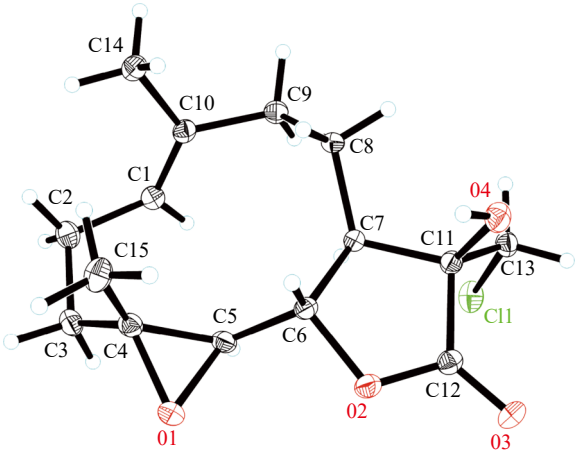

Fig. 7 X-ray crystallographic structure of 2 (CCDC: 2239028).

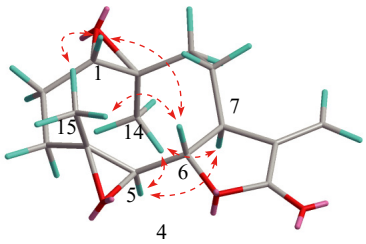

Fig. 8 The key NOESY correlations of 4.

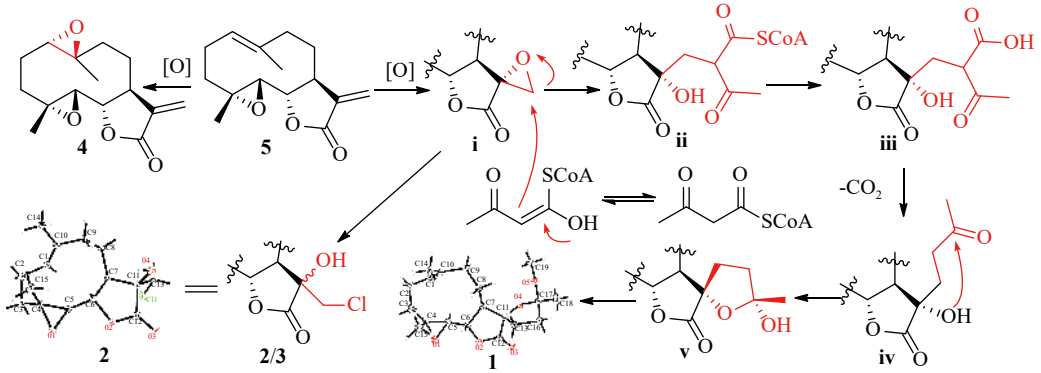

Scheme 1 Speculated biosynthetic pathway of compounds 1–4.

14 with H-5, and H-5 with H-7. Therefore, the structure of magrandate D (**4**) was confidently assigned.

To ascertain whether the three novel compounds (**1**–**3**) were inherent components of the plant, liquid chromatography-mass spectrometry (LC-MS) analysis was performed on both the crude extracts and the isolated novel compounds. The analysis results confirmed that these rare compounds (**1**–**3**) were indeed present in the crude extract of the plant.

A plausible biosynthetic pathway for the three rare gemarane-type SLs (**1**–**3**) originating from compound **5** was proposed. As illustrated in Scheme 1, compound **5** is hypothesized to undergo enzymatic epoxidation reactions at $\Delta^{11,13}$ and $\Delta^{1,10}$, leading to the formation of intermediate i and compound **4**, respectively [22]. The 11,13-epoxy ring in intermediate **i** is proposed to open under the action of halohydrin dehalogenase, resulting in the production of two rare chlorine-substituted parthenolide analogs (**2**/**3**) [23]. Regarding compound **1**, the 11,13-epoxy moiety in intermediate **i** is believed to undergo a nucleophilic attack by acetoacetyl-CoA (coenzyme A), forming a critical intermediate **ii** [24]. This intermediate **ii** would then undergo oxidation to produce intermediate **iii**, which subsequently experiences decarboxylation and an intermolecular nucleophilic addition, culminating in the formation of the novel spiro ring system (**v**) [25]. The final step in the synthesis of compound **1** involves methylation of the hydroxyl group in intermediate **v**.

The anti-inflammatory activities of all isolated compounds were evaluated in RAW264.7 cells at varying concentrations of 0.1, 1, 10, and 100 μmol·L^{-1} [26-28]. The results demonstrated that all isolates effectively inhibited nitric oxide (NO) production, with the inhibition rate ranging from 20% to 88.7%, and importantly, without exhibiting cytotoxicity (Fig. 9). Among these, four compounds (**2**–**5**) exhibited the most significant activity and were selected for further detailed study. Their half-maximal inhibitory concentration (IC_{50}) values varied from 0.79 to 51.77 μmol·L^{-1} (Table 2). Of particular note, three compounds (**3**–**5**) displayed more potent inhibitory activities [IC_{50} 0.79–4.73 μmol·L^{-1}] than the positive control, pyrrolidine dithiocarbamate (PDTC), which had an IC_{50} of 5.68 μmol·L^{-1}. Specifically, compound **5** showed an anti-inflammatory effect with an IC_{50} 0.79 μmol·L^{-1}, which was 7.2 times more potent than that of PDTC. An interesting observation was made with compounds **2** and **3**, which are a pair of epimers. Despite their structural similarity, they exhibited different levels of activity. Compound **3**, possessing an *α*-oriented chloromethyl group, was found to be 10.9 times more active than compound **2**, which has a *β*-oriented chloromethyl group. This notable difference in activity between the epimers highlights the significant impact of stereochemistry on the biological activity of these compounds.

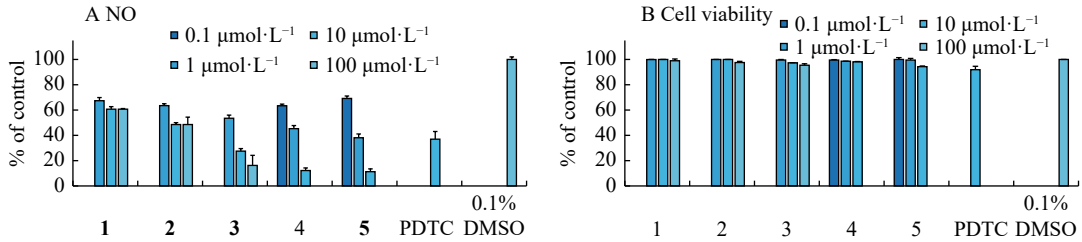

Fig. 9 (A) Inhibitory effects of compounds 1–5 against NO production in LPS-stimulated RAW264.7 cells. (B) Cytotoxicity of compounds 1–5 on RAW264.7 cells. The data are expressed as mean ± SEM (n = 3). $^{*}P < 0.05$, $^{**}P < 0.01$ *vs* DMSO group.

Table 2 Inhibition of nitric oxide production of 2–5

Compound	IC_{50} (μmol·L^{-1})
2	51.77 ± 3.26
3	4.73 ± 0.24
4	1.03 ± 0.02
5	0.79 ± 0.05
PDTC[a]	5.68 ± 0.53

[a]Pyrrolidine dithiocarbamate is used as a positive control.

The cytotoxic activities of all isolated compounds were assessed against three tumor cell lines using the MTT (methylthialazole tetrazolium) assay [29-30]. These cell lines included HCT-116 (human colon cancer cells), Colo320DM (human colorectal adenocarcinoma cells), and HEL (human erythroleukemia cells). Among the isolates, compounds **4** and **5** demonstrated moderate cytotoxic activities against these cancer cell lines. The half-maximal inhibitory concentration (IC_{50}) values for these compounds ranged from 3.09 to 11.23 μmol·L^{-1} (Table 3). This evaluation highlights the potential of compounds **4** and **5** as candidates for further exploration in cancer therapeutics, given their observed efficacy in inhibiting the proliferation of a variety of cancer cell lines. The moderate cytotoxic activity observed suggests that these compounds could be of interest for future drug development and research in the field of oncology.

Table 3 Cytotoxic activities of compounds 1–5[a]

Compound	IC_{50} (μmol·L^{-1})		
	HCT-116	Colo320DM	HEL
4	9.11 ± 1.40	11.23 ± 1.39	4.57 ± 0.13
5	8.59 ± 0.25	8.37 ± 0.94	3.09 ± 0.13
ADR[b]	0.20 ± 0.13	5.81 ± 0.34	0.14 ± 0.03

[a] Compounds **1**–**3** was inactive at the concentration of 20 μmol·L^{-1}.
[b] ADR: adriamycin is used as a positive control.

Conclusion

This research successfully isolated four new sesquiterpenes, including three novel sesquiterpene lactones (SLs) (compounds **1**–**3**) and a new compound (**4**), along with a biosynthetically related compound (**5**), from the leaves of *Magnolia grandiflora*. Architecturally, Magrandate A (compound **1**) is particularly noteworthy as it represents the first C18 homogermacranolide, featuring a unique 1,7-dioxaspiro[4.4]nonan-6-one core structure. Magrandates B and C (compounds **2** and **3**) are distinguished as rare chlorine-substituted parthenolide analogs. Analysis of the biogenic synthesis pathways suggests that compounds **1**–**4** are derivatives of compound **5**, with differing structural outcomes based on the epoxidation at $\Delta^{11,13}$ or $\Delta^{1,10}$ positions in compound **5**. This leads to the formation of diverse structures among compounds **1**–**4**. Specifically, the C17-type homogermacranolide (compound **1**) is biosynthesized from compound **5** through a sequence of reactions, including epoxidation, nucleophilic addition involving acetoacetyl-CoA, and dihydroxylation processes. The discovery of these compounds, especially with such unique structural features and biological activities, contributes significantly to the field of natural product chemistry and offers potential leads for the development of new therapeutic agents.

Experimental

General information

The methodologies employed in the analytical and preparative procedures of this study were comprehensive and state-of-the-art, ensuring precise and reliable data for the characterization of the isolated compounds. The optical rotations and ECD data were measured using an Autopol IV automatic polarimeter and a JASCO-810 polarimeter, respectively. These instruments are highly sensitive and accurate for determining the optical properties of chiral molecules. The ^{1}H, ^{13}C NMR, and 2D NMR spectra, essential for elucidating the structures of the compounds, were obtained using a Bruker Advance NEO 600 spectrometer. Tetramethylsilane (TMS) served as the internal standard, providing a reliable reference point for chemical shift measurements. The ESI-MS and HR-ESI-MS analyses, which are crucial for determining the molecular weights and formulas of the compounds, were recorded on an Agilent 1100 instrument and a Thermo ultimate 3000/Q EXACTIVE FOCUS mass spectrometer, respectively. For additional optical rotation measurements, a JASCOP-1020 polarimeter was utilized. UV spectra, which can offer insights into the conjugated systems of the compounds, were acquired using a Shimadzu UV-2401PC spectrometer. Infrared (IR) spectra, useful for identifying functional groups, were obtained on a Bruker FT-IR Tensor-27 and iCAN 9 infrared spectrophotometer using KBr disks. Column chromatography, a key step in the purification process, was conducted using a variety of stationary phases: silica gel (300–400 mesh; Qingdao Marine Chemical Co., Ltd., China), MCI gel CHP20P (Mitsubishi Chemical Industries Ltd.), RP-C18 gel (40–63 μm, Merck, Darmstadt, Germany), and Sephadex LH-20 (40–70 μm, Amersham Pharmacia Biotech AB, Uppsala, Sweden). Semi-preparative high-performance liquid chromatography (HPLC) was performed using a system composed of a Hanbon NP7005c controller, a Hanbon NP7005 pump, and a Hanbon NU3000c dual λ absorbance detector, equipped with a YMC-Triart-C18 column (250 mm × 10.0 mm, 5 μm). Fractions were monitored by thin-layer chromatography (TLC) on GF_{254} plates (Qingdao Marine Chemical Co., Ltd.). All other reagents used in the study were of analytical grade or guaranteed reagent quality and were employed without further purification, ensuring the accuracy and reproducibility of the experimental results.

Plant material

The collection of *Magnolia grandiflora* leaves was conducted in Libo County, located in the Guizhou Province of China. The identification of this plant material was expertly carried out by Mr. HOU Xiaoqi, ensuring the accuracy and reliability of the botanical source used in the study. For reference and verification purposes, a voucher specimen of this plant, bearing the number 20201015, has been deposited in the Natural Products Research Center of Guizhou Province. This documentation and deposition of the voucher specimen are crucial steps in phytochemical research. They provide a tangible reference for future studies and aid in the reproducibility of the research by allowing other scientists to reference or access the exact botanical material used. The association with a well-established institution like the Key Laboratory of Chemistry for Natural Products of Guizhou Province and the Chinese Academy of Sciences further adds credibility and scientific rigor to the study.

Extraction, isolation, and purification

The air-dried and pulverized leaves of *M. grandiflora* (30.0 kg) were extracted with 150 L 90% MeOH under reflux three times (3 h each time). The final MeOH extracts were combined and concentrated under vacuum to obtain a crude residue (2.1 kg), which was chromatographed on a silica gel column (200–300 mesh) eluted with petroleum ether−acetone (99 ∶ 1→0 ∶ 100, *V*/*V*) to yield 13 fractions (Frs. A–M).

Fraction G (244.5 g) underwent further separation into 15 subfractions (Frs. G1–G15) using an MCI column and a gradient of MeOH and water (from 50 ∶ 50 to 100 ∶ 0, *V*/*V*). Subfraction G6 (12.5 g) was chromatographed over a silica gel column (300–400 mesh) with a gradient of petroleum ether and dichloromethane (CH_2C_{l2}), followed by dichloromethane and ethyl acetate (EtOAc), resulting in 14 subfractions (Frs. G6a–G6n). Subfraction G6h (800.7 mg) was further purified using a Sephadex LH-20 column (MeOH) and a silica gel column (petroleum ether–EtOAc 90 ∶ 10, *V*/*V*), leading to the isolation of compound **1** (6.7 mg). Fraction G8 (20.0 g) was separated using a silica gel column (CH_2C_{l2}–acetone), yielding Frs. G8a and G8b. Fr. G8a was then subjected to HPLC purification (MeOH–H_2O, 50 ∶ 50,

V/*V*, 3.0 mL·min^{-1}) to obtain compounds **4** (15.1 mg, t_R = 15.5 min) and **5** (20.1 mg, t_R = 15.5 min). Compounds **2** (18.3 mg) and **3** (24.5 mg) were isolated from Fraction G9 (8.4 g) after repeated chromatography on a silica gel column.

*Magrandate A (**1**)*: colorless needles; $[\alpha]_D^{25}$ −50.9 (*c* 0.20, MeOH); UV (MeOH) λ_{max} (log ε) 200 (0.65) nm; IR (KBr) ν_{max} 2358, 2342, 1716, 1682, 1557, 1507 cm^{-1}; ^{1}H NMR ($CDCl_3$, 600 MHz) and ^{13}C NMR ($CDCl_3$, 150 MHz) data (Table 1); (+)-HR-ESI-MS *m/z* 359.1827 [M + Na]$^+$ (Calcd. for $C_{19}H_{28}O_5Na$, 359.1829).

Crystal data for **1**: $C_{19}H_{28}O_5$, (*M* = 336.41 g·mol^{-1}): orthorhombic, space group $P2_12_12_1$ (no. 19), *a* = 7.9742(2) Å, *b* = 11.1488(3) Å, *c* = 20.2719(6) Å, *V*= 1802.23(8) Å^3, *Z* = 4, *T* = 169.99(10) K, μ(Cu Kα) = 0.721 mm^{-1}, *Dcalc* = 1.240 g·cm^{-3}, 10106 reflections measured (8.724° ≤ 2Θ ≤ 147.918°), 3567 unique (R_{int} = 0.0376, R_{sigma} = 0.0356) which were used in all calculations. The final R_1 was 0.0349 (I > 2σ(I)), and wR_2 was 0.0887 (all data). CCDC: 2239027

*Magrandate B (**2**)*: colorless needles; $[\alpha]_D^{25}$ +37.3 (*c* 0.27, MeOH); UV (MeOH) λ_{max} (log ε) 199 (0.603) nm; IR (KBr) ν_{max} 2926, 2358, 1771, 1652, 1557, 1540, 1506, 1456, 1260 cm^{-1}; ^{1}H NMR ($CDCl_3$, 600 MHz) and ^{13}C NMR ($CDCl_3$, 150 MHz) data (Table 1); (+)-HR-ESI-MS *m/z* 323.1015 [M + Na]$^+$ (Calcd. for $C_{15}H_{21}O_4Cl$, 323.1021).

Crystal data for **2**: $C_{15}H_{21}ClO_4$, (*M* = 300.77 g·mol^{-1}): orthorhombic, space group $P2_12_12_1$ (no. 19), *a* = 7.61740(10)Å, *b* = 8.65720(10)Å, *c* = 21.9959(3)Å, *V* = 1450.53(3)Å^3, *Z* = 4, *T* = 169.99(10)K, μ(Cu Kα) = 2.432 mm^{-1}, *Dcalc* = 1.377 g·cm^{-3}, 7768 reflections measured (8.04° ≤ 2Θ ≤ 148.036°), 2886 unique (R_{int} = 0.0519, R_{sigma} = 0.0419) which were used in all calculations. The final R_1 was 0.0428 (I > 2σ(I)), and wR_2 was 0.1192 (all data). CCDC: 2239028.

*Magrandate C (**3**)*: colorless oil; $[\alpha]_D^{25}$ −56.0 (*c* 0.18, MeOH); UV (MeOH) λ_{max} (log ε) 200 (1.23) nm; IR (KBr) ν_{max} 2927, 2358, 1780, 1652, 1457, 1145 cm^{-1}; ^{1}H NMR ($CDCl_3$, 600 MHz) and ^{13}C NMR ($CDCl_3$, 150 MHz) data (Table 1); (+)-HR-ESI-MS *m/z* 323.1015 [M + Na]$^+$ (Calcd. for $C_{15}H_{21}O_4Cl$, 323.1021).

Magrandate D (**4**): colorless needles; $[\alpha]_D^{25}$ +56 (*c* 0.26, MeOH); UV (MeOH) λ_{max} (log ε) 201 (1.03) nm; IR (KBr) ν_{max} 2937, 1772, 1453, 1393, 1300, 1264, 1134, 1002 cm^{-1}; UV (MeOH) λ_{max} (log ε) 201 (3.53) nm; ^{1}H NMR ($CDCl_3$, 600 MHz) and ^{13}C NMR ($CDCl_3$, 150 MHz) data (Table 1); (+)-HR-ESI-MS *m/z* 287.1261 [M + Na]$^+$ (Calcd. for $C_{15}H_{20}O_4Na$, 287.1254).

Theoretical ECD calculation

Conformers with a Boltzmann population exceeding 5% were chosen for ECD calculations. This step ensures that only the most statistically significant conformers (those contributing significantly to the overall conformational ensemble) were considered, enhancing the accuracy of the ECD predictions. The selected conformers were initially optimized using the B3LYP/6-31g(d,p) level of theory. The optimization was conducted in methanol (MeOH) using the Polarizable Continuum Model (PCM) [18-20] for solvent effects. This level of theory is a common choice for quantum chemical calculations, offering a good balance between computational cost and accuracy. The ECD calculations were performed in MeOH using Time-dependent Density Functional Theory (TD-DFT) at the B3LYP/6-31+g(d,p) level. This approach is widely used in computational chemistry for studying excited states and optical properties of molecules. Rotatory strengths for the three most excited states were calculated for all conformers of compounds **1** and **2**. These strengths are essential for predicting the ECD spectra, as they reflect the molecule's ability to rotate plane-polarized light. The ECD spectra were generated using SpecDis 1.71 (University of Würzburg, Würzburg, Germany) and GraphPad Prism 5 (University of California San Diego, USA). This was accomplished by applying Gaussian band shapes with a sigma of 0.3 eV to the dipole-length rotational strengths. The use of these software tools allows for the visualization and analysis of the calculated ECD spectra, facilitating comparison with experimental data. Overall, this methodology reflects a comprehensive and sophisticated approach to determining the absolute configuration of chiral molecules through ECD calculations, leveraging advanced computational techniques and software.

X-ray crystallographic analysis

Colorless block crystals of compounds **1** and **2** were obtained from a methanol (MeOH) solution after storage in a 3 °C refrigerator for two weeks. These crystals were examined using a Bruker Apex Duo diffractometer with Cu Kα radiation, a standard technique for determining crystal structures. The structures were refined using full-matrix least-squares on F^2 using the SHELXL-97 software [21], a widely recognized program for crystallographic computation. Additional parameters and data related to these analyses can be found in the supporting information for the research article.

Inhibition of nitric oxide production assay

The assay was performed as described previously [26-27]. Each compound was dissolved in DMSO and then further diluted in a medium to achieve various concentrations. NO production was measured using the Griess reagent assay. This involved adding 100 μL of Griess reagents A and B to 100 μL of supernatant from LPS (lipopolysaccharide) or compound-treated cells in triplicate [28]. After incubation for 5 min, absorbance was measured at 570 nm using a 2104 Envision multilabel plate reader (Perkin−Elmer Life Sciences, Inc., Boston, MA, USA). Cytotoxicity was determined using the MTT assay, with PDTC serving as a positive control.

Cytotoxic activity experiment

The experiment was conducted as described previously [29, 30]. Cells were cultured in RPMI-1640 (HEL and HCT116) or DMEM (MDA-MB-231) medium supplemented with 5% fetal bovine serum (FBS) and 1% ampicillin/streptomycin. MTT assay was employed to evaluate the cytotoxicity of all compounds. Cells were seeded in 96-well plates and treated with different concentrations of the derivatives for 72 h. Absorbance at 490 nm was measured using a Vari-

oskan LUX microplate reader (Thermo, USA). The half-maximal inhibitory concentration (IC_{50}) was calculated based on the relative survival curve. All experiments were performed in triplicates and repeated at least three times to ensure reliability.

Supplementary Information

Supplementary data to this article can be obtained by sending E-mail to the corresponding authors.

References

[1] Hotamisligil GS. Inflammation and metabolic disorders [J]. *Nature*, 2006, **444**: 860-867.

[2] Leng F, Edison P. Neuroinflammation and microglial activation in Alzheimer disease: where do we go from here [J]. *Nat Rev Neurol*, 2021, **17**: 157-172.

[3] Freeman L, Guo H, David CN, *et al*. NLR members NLRC4 and NLRP3 mediate sterile inflammasome activation in microglia and astrocytes [J]. *J Exp Med*, 2017, **214**: 1351-1370.

[4] Labzin LI, Heneka MT, Latz E. Innate immunity and neurodegeneration [J]. *Annu Rev Med*, 2018, **69**: 437-449.

[5] Monteiro C, Silvestre S, Duarte AP, *et al*. Safety of non-steroidal anti-inflammatory drugs in the elderly: an analysis of published literature and reports sent to the portuguese pharmacovigilance system [J]. *Int J Environ Res Public Health*, 2022, **19**: 3541.

[6] Zeng YR, Li YN, Zhang ZZ, *et al*. Hypermoins A–D: rearranged nor-polyprenylated acylphloroglucinols from the flowers of *Hypericum monogynum* [J]. *J Org Chem*, 2021, **86**: 7021-7027.

[7] Chadwick M, Trewin H, Gawthrop F, *et al*. Sesquiterpenoids lactones: benefits to plants and people [J]. *Int J Mol Sci*, 2013, **14**: 12780-12805.

[8] Galindo JC, de Luque AP, Jorrín J, *et al*. SAR studies of sesquiterpene lactones as *Orobanche cumana* seed germination stimulants [J]. *J Agric Food Chem*, 2002, **50**: 1911-1917.

[9] Raupp FM, Spring O. New sesquiterpene lactones from sunflower root exudate as germination stimulants for *Orobanche cumana* [J]. *J Agric Food Chem*, 2013, **61**: 10481-10487.

[10] Cho HM, Park EJ, Park YJ, *et al*. Sesquiterpene lactone and its unique proaporphine hybrids from *Magnolia grandiflora* L. and their anti-inflammatory activity [J]. *Phytochemistry* 2022, **200**: 113211.

[11] El-Feraly FS, Chan YM. Isolation and characterization of the sesquiterpene lactones costunolide, parthenolide, costunolide diepoxide, santamarine, and reynosin from *Magnolia grandiflora* L. [J]. *J Pharm Sci*, 1978, **67**: 347-350.

[12] Chang HS, Lee SJ, Yang CW, *et al*. Cytotoxic sesquiterpenes from *Magnolia kachirachirai* [J]. *Chem Biodivers*, 2010, **7**: 2737-2747.

[13] Matos MS, Anastácio JD, Santos NDC. Sesquiterpene lactones: promising natural compounds to fight inflammation [J]. *Pharmaceutics*, 2021, **13**: 991.

[14] Ma FF, Hu ZX, Chen J, *et al*. Chemical constituents of the leaves of *Magnolia grandiflora* Linn. and their antitumor activities [J]. *Chin Pharm J*, 2016, **51**: 967-971.

[15] Wu SH, Luo XD, Ma YB, *et al*. Two new germacranolides from *Magnolia grandiflora* [J]. *J Asian Nat Prod Res*, 2001, **2**: 95-102.

[16] Ding LF, Su J, Pan ZH, *et al*. Cytotoxic sesquiterpenoids from the leaves of *Magnolia grandiflora* [J]. *Phytochemistry*, 2018, **155**: 182-190.

[17] Yang MH, Blunden G, Patel AV, *et al*. Coumarins and sesquiterpene lactones from *Magnolia grandiflora* leaves [J]. *Planta Med*, 1994, **60**: 390.

[18] Zhang Q, Zan YH, Yang HG, *et al*. Anti-tumor alkaloids from *Peganum harmala* [J]. *Phytochemistry*, 2022, **197**: 113107.

[19] Grimblat N, Zanardi MM, Sarotti AM. Beyond DP4: an improved probability for the stereochemical assignment of isomeric compounds using quantum chemical calculations of NMR shifts [J]. *J Org Chem*, 2015, **80**: 12526-12534.

[20] Xin D, Jones PJ, Gonnella NC. DiCE: diastereomeric in silico chiral elucidation, expanded DP4 probability theory method for diastereomer and structural assignment [J]. *J Org Chem*, 2018, **83**: 5035-5043.

[21] Cao MM, Zhang Y, Li XH, *et al*. Cyclohexane-fused octahydroquinolizine alkaloids from *Myrioneuron faberi* with activity against hepatitis C virus [J]. *J Org Chem*, 2014, **79**: 7945-7950.

[22] May SW. Enzymatic epoxidation reactions [J]. *Enzyme Microb Technol*, 1979, **1**: 15-22.

[23] Schallmey A, Schallmey M. Recent advances on halohydrin dehalogenases-from enzyme identification to novel biocatalytic applications [J]. *Appl Microbiol Biotechnol*, 2016, **100**: 7827-7839.

[24] Xiong J, Wang LJ, Qian J, *et al*. Structurally diverse sesquiterpenoids from the endangered ornamental plant *Michelia shiluensis* [J]. *J Nat Prod*, 2018, **81**: 2195-2204.

[25] Han JJ, Zhang JZ, Zhu RX, *et al*. Plagiochianins A and B, two *ent*-2,3-*seco*-aromadendrane derivatives from the liverwort *Plagiochila duthiana* [J]. *Org Lett*, 2018, **20**(20): 6550-6553.

[26] Yoon SB, Lee YJ, Park SK, *et al*. Anti-inflammatory effects of *Scutellaria baicalensis* water extract on LPS-activated RAW 264.7 macrophages [J]. *J Ethnopharmacol*, 2009, **125**: 286-290.

[27] Li H, Wang L, Yang Z, *et al*. Kadsuralignans H-K from *Kadsura coccinea* and their nitric oxide production inhibitory effects [J]. *J Nat Prod*, 2007, **70**: 1999-2002.

[28] Choi HG, Lee DS, Li B, *et al*. Santamarin, a sesquiterpene lactone isolated from *Saussurea lappa*, represses LPS-induced inflammatory responses *via* expression of heme oxygenase-1 in murine macrophage cells [J]. *Int Immunopharmacol*, 2012, **13**: 271-279.

[29] Wang F, Hua HM, Pei YH, *et al*. Triterpenoids from the resin of *Styrax tonkinensis* and their antiproliferative and differentiation effects in human leukemia HL-60 Cells [J]. *J Nat Prod*, 2006, **69**: 807-810.

[30] Li Y, Qiu J, Yi P, *et al*. Isolation and synthesis of rocaglaol derivatives by inhibiting Wnt/*β*-catenin and MAPK signaling pathways against colorectal cancer [J]. *Bioorg Chem*, 2022, **129**: 106149.

Cite this article as: XU Shuangyu, ZHANG Feng, TAO Linlan, JIANG Yangming, HUANG Tao, LI Yanan, HU Zhanxing, YANG Jue, HAO Xiaojiang, YUAN Chunmao. Three rare anti-inflammatory sesquiterpene lactones from *Magnolia grandiflora* [J]. *Chin J Nat Med*, 2024, **22**(3): 265-272.